Molecular Catalysis 475 (2019) 110457

Contents lists available at ScienceDirect

Molecular Catalysis

journal homepage: www.elsevier.com/locate/mcat

Probing into the effects of cluster size and Pd ensemble as active center on the activity of H_2 dissociation over the noble metal Pd-doped Cu bimetallic clusters

Riguang Zhang*, Ying Wang, Baojun Wang*, Lixia Ling

Key Laboratory of Coal Science and Technology of Ministry of Education and Shanxi Province, Taiyuan University of Technology, Taiyuan 030024, Shanxi, PR China

ARTICLE INFO

Keywords:
Pd-doped Cu catalyst
H_2 dissociation
Cluster size
Pd ensemble
Density functional theory

ABSTRACT

Aiming at probing into the effects of cluster size and Pd ensemble as active center on H_2 dissociation over Pd-doped Cu bimetallic cluster, density functional theory calculations are employed to investigate H_2 adsorption and dissociation over the Cu and Pd-doped Cu clusters with different sizes. The results show that compared to Cu cluster, the doped Pd atom and its ensemble composed of outermost layer and its connected sub-layer Pd atoms as active center greatly enhance catalytic activity of H_2 dissociation at the same size of Pd-doped Cu clusters, which is attributed to the interaction enhancement between H_2 and the clusters since *d*-band centers gradually approach the Fermi level and the electron-rich regions are formed around Pd ensemble. Moreover, among the Pd-doped Cu clusters with different sizes, the Bader charge indicate that when the number of doped-Pd atoms is same, the amount of charge on Pd ensemble increases with the size increasing of Pd-doped Cu catalysts, the cluster with larger size is beneficial for promoting the activity of H_2 dissociation; thus, the size effect of Pd-doped Cu cluster on H_2 dissociation is dominantly attributed to the electronic effect. This work not only provides a valuable clue for evaluating catalytic activity of other promoter metal-doped Cu catalysts for H_2 dissociation, but also gives out the ways that adjusting the cluster size and the promoter ensemble can facilitate the dissociation of H_2 atoms as an initially key step in the heterogeneous hydrogenation.

1. Introduction

In the heterogeneous catalytic reactions, the bimetallic catalysts composed of the precious metal alloyed with inert metal have attracted more attention and play a key role, in which a limited number of noble metal atoms usually form the ensemble to perform as the active centers [1–4]. Thus, in order to illustrate and improve the catalytic ability of active centers, it is necessary to identify the configurations and properties of the ensemble performed as catalytic active centers [5–10]. Nowadays, the inexpensive Pd-doped Cu catalysts were widely used in catalytic hydrogenation, such as CO_2 hydrogenation [11–13], syngas conversion [14–16], C_2H_2 selective hydrogenation [17–19], and so on. Among these reactions, H_2 dissociation as the initial step can provide enough hydrogen sources for the hydrogenation reactions.

Up to now, extensive studies have theoretically and experimentally indicated that Cu(111) surface doped with noble metal Pd atoms is able to promote H_2 dissociation with better catalytic activity [20–25]. Meanwhile, the experiments have observed that in the preparation process of Pd-doped Cu catalyst, part of Pd deposited into the sub-layer of Cu catalyst [26–28], namely, Pd atoms exist at the outermost layer and sub-layer of Pd-doped Cu catalysts. Further, density functional theory (DFT) calculations by Fu et al. [3] also found that the Pd ensemble as active centers formed by the outermost layer and connected sub-layer Pd atoms obviously improve catalytic activity of H_2 dissociation over the Cu(111) surface doped with Pd atoms.

On the other hand, Nano-metal clusters have been widely used because of their large specific surface area and high surface atomic unsaturation, and so on. Extensive studies [29–31] indicated experimentally and theoretically that the catalytic performance can be changed by the geometric size of nano-metal cluster. Zhao et al. [32] proved that the activity of Cu cluster is closely related to its size for C_2H_2 selective hydrogenation, Cu cluster with the large size exhibits high selectivity towards gaseous C_2H_4 formation. Zhang et al. [33] found that the cluster size of Cu catalyst affects the optimal path of CH_x formation in syngas conversion. Wörz et al. [34] investigated the CO + NO reaction on Pd_n($n < 30$) clusters, indicating that both molecularly bonded and dissociated NO co-exist on the larger Pd clusters, while NO is dissociated on the smaller Pd clusters. Kunz et al. [35] observed that

* Corresponding authors.
E-mail addresses: zhangriguang@tyut.edu.cn (R. Zhang), wangbaojun@tyut.edu.cn, wbj@tyut.edu.cn (B. Wang).

https://doi.org/10.1016/j.mcat.2019.110457
Received 17 March 2019; Received in revised form 7 May 2019; Accepted 2 June 2019
Available online 14 June 2019

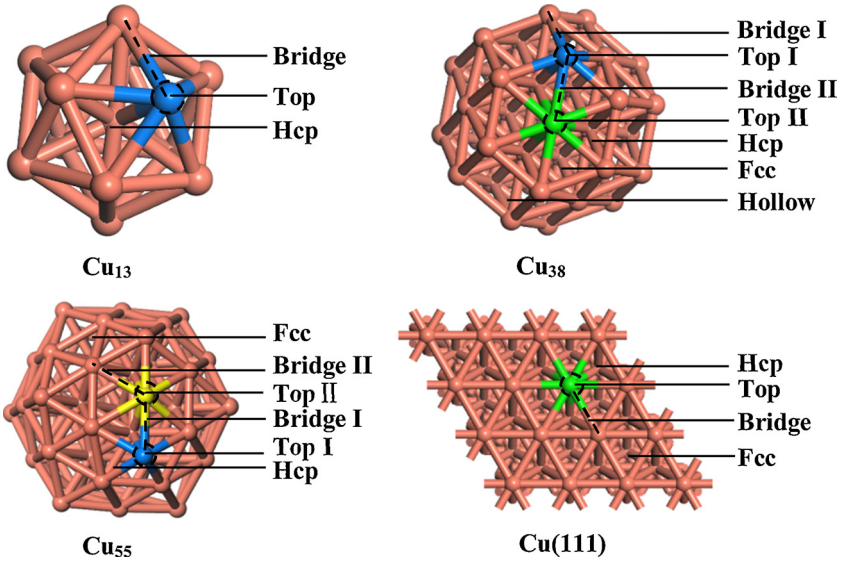

Fig. 1. The optimized structures and adsorption sites for the Cu_{13}, Cu_{38}, Cu_{55} clusters and the Cu(111) surface. The blue, yellow and green atoms correspond to 6-, 8- and 9-coordination Cu atoms, respectively. (For interpretation of the references to colour in this figure legend, the reader is referred to the web version of this article.)

oxygen activation occurs easily and CO adsorption is weakened over the smaller Pd clusters. Further, H_2 dissociation easily occurs on Pt_{13} cluster compared to other Pd_n(n = 4, 6, 19, 55) clusters [36]. However, up to now, as far as we know, except for the reported studies by Fu et al. [3] about H_2 dissociation over the Pd-doped periodic Cu(111) surface representing the much larger size cluster, few studies over the Pd-doped Cu cluster catalysts are carried out to explore the size effects on H_2 dissociation, and therefore little information was known for the effects of cluster size and Pd ensemble as active center on the activity of H_2 dissociation. In consequence, it is worth to further understand the intrinsic electronic and geometric properties for the Pd-doped Cu cluster with different sizes, and the activity of H_2 dissociation.

The present DFT study is designed to investigate H_2 adsorption and dissociation over Pd-doped Cu nano-cluster with different sizes compared to the corresponding Cu catalysts. Pd-doped Cu_n(n = 13, 38, 55) clusters and Pd-doped Cu(111) surface are employed to present the Pd-doped Cu nano-cluster catalysts with different sizes. Different forms of Pd ensemble are presented using the structures of single Pd atom doped into the outermost layer and those of Pd ensemble formed by the outermost layer and its connected sub-layer Pd atoms. The comparisons between the Cu and Pd-doped Cu clusters with different sizes are carried out to obtain the effects of cluster size and Pd ensemble as active center on H_2 dissociation. This work is hoped to provide an effective way for improving catalytic performance of Pd-doped Cu nano-clusters in H_2 dissociation by controlling cluster size and Pd ensemble.

2. Computational details

2.1. Computational method

DFT calculations were performed using $Dmol^3$ code [37,38]. GGA functional treated by PBE functional were selected to describe the electron interactions [39,40]. The DNP polarization function was used as a basis set for valence electron function of all computational atoms. An effective core potential (ECP) is performed for the inner electrons of metal atoms; while the all electron basis set is used for the H atoms and H_2 molecule. The surface Brillouin zone is selected as $2 \times 2 \times 1$ *k*-points and 0.005 Ha is set for smearing value.

The transition states (TS) were identified by the method of complete LST/QST [39,41] for H_2 dissociation. In order to validate the accuracy of transition state, TS confirmation and frequency analysis were calculated, the transition state with the single imaginary frequency is directly connected to the reactant and product. The zero-point energy [42] can be also obtained.

The adsorption free energies of H atoms and H_2 molecule (G_{ads}) including zero-point energy correction are defined according to the Eq. (1):

$$G_{ads} = E_{(T)} - E_{(catalyst)} - E_{(species)} + G_{(T)} - G_{(catalyst)} - G_{(species)} \quad (1)$$

Where $E_{(catalyst)}$ is the energy of the catalyst, $E_{(species)}$ represents the energy of H atoms or H_2 species in the gas phase, and $E_{(T)}$ is the total energies of the adsorbed system. $G_{(catalyst)}$, $G_{(species)}$ and $G_{(T)}$ are the corresponding Gibbs free energies at a finite temperature.

The activation barrier (ΔG_a) and reaction energy (ΔG) considered at a finite temperature are calculated according to the Eqs. (2) and (3):

$$\Delta Ga = E_{TS} - E_R + G_{TS} - G_R \quad (2)$$

$$\Delta G = E_P - E_R + G_P - G_R \quad (3)$$

Where E_R, E_{TS} and E_P correspond to the total energies of the slab along with adsorbed H_2, the transition state and the dissociated H atoms, respectively. G_R, G_{TS} and G_p are the corresponding value of Gibbs free energies at a finite temperature.

In order to better simulate the realistic hydrogenation reaction temperature, we set the temperature to 475 K according to the reaction temperature range for three types of typical reactions involved in CO_2 hydrogenation (380–523 K) [11–13], syngas conversion (473–583 K) [14,16] and C_2H_2 selective hydrogenation (373–530 K) [17–19,43,44].

2.2. Surface model

In this study, as shown in Fig. 1, different sizes of Cu catalysts are modeled using the Cu_{13}, Cu_{38} and Cu_{55} nanoclusters with high symmetry, the corresponding diameter size are 4.95, 7.60 and 9.77 Å, respectively. Meanwhile, the much larger size of Cu catalysts are represented using the Cu(111) periodic surface.

Cu catalysts doped with Pd are constructed by substituting the outermost layer or sub-layer Cu atoms with Pd atoms, they are stable energetically [45,46]. Moreover, the outermost layer and sub-layer replacement affect the catalytic performance. Hence, in this study, for the Pd-doped Cu cluster with different sizes, the structures of individual Pd atom at the outermost layer and that formed by Pd atoms at the outermost layer and its connected sub-layer are considered, the stable configurations of these structures are shown in Fig. 2.

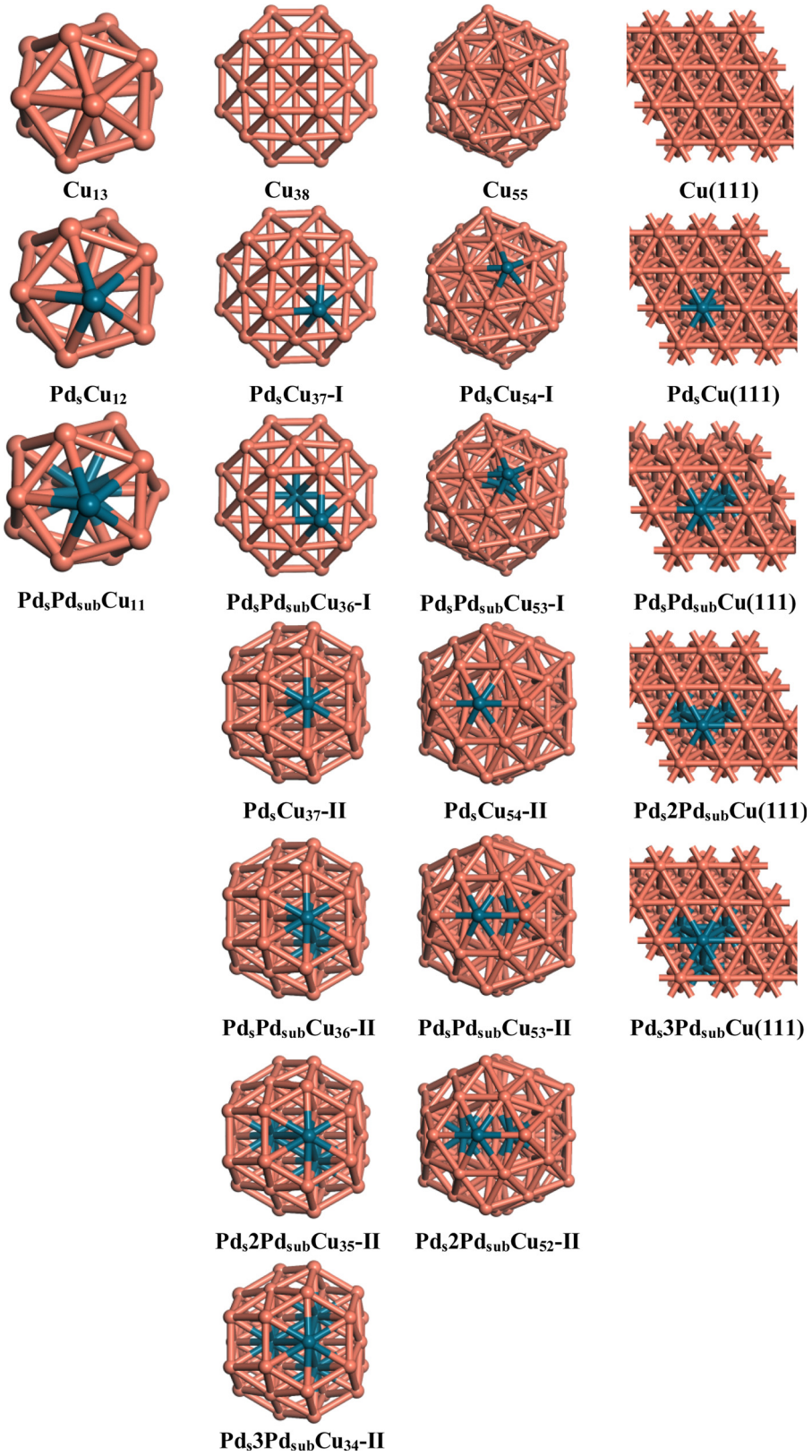

Fig. 2. The optimized structures for different sizes of the pure Cu and Pd-doped Cu clusters. The blue and orange atoms correspond to Pd and Cu atoms, respectively. (For interpretation of the references to colour in this figure legend, the reader is referred to the web version of this article.)

For the Cu_{13} and Pd-doped Cu_{13} clusters, the icosahedral structure of Cu_{13} cluster is the most stable with the outmost layer corresponding to twenty (111) facets of 12 atoms and an inner core of an atom [47–50]. Meanwhile, the shell of Cu_{13} cluster has only 6-coordination Cu atoms. Thus, when the single Pd atom is doped into the outermost layer of Cu_{13} cluster, only one type of structure exists, which is named as Pd_sCu_{12}. Accordingly, there is one type of Pd ensemble formed by an outermost layer and a core Pd atoms, denoted as $Pd_sPd_{sub}Cu_{11}$. Top,

Bridge and Hcp sites exist.

For the Cu_{38} and Pd-doped Cu_{38} clusters, Cu_{38} is the truncated octahedron including Cu(111) and Cu(100) planes [51–53]. Unlike Cu_{13}, the Cu_{38} inner core consists of an octahedron with 6 atoms and the shell consists of 32 atoms. Among the shell Cu atoms, there are 6-coordination and 9-coordination Cu atoms. Fig. 1 shows seven adsorption sites of Cu_{38} cluster. Since Top I and Top II have different coordination numbers of 6 and 9 in Cu_{38} cluster, respectively, two types of replacement for the shell Cu atoms exist, one is to replace 6-coordination Cu atom to form Pd_sCu_{37}-I, and the other is to replace 9-coordination Cu atom to form Pd_sCu_{37}-II. Further, for Pd_sCu_{37}-I, the inner core Pd atom replacement model is $Pd_sPd_{sub}Cu_{36}$-I. For Pd_sCu_{37}-II, up to three inner layer Pd atoms can be replaced to connect with the shell Pd atom, which are named as $Pd_sPd_{sub}Cu_{36}$-II, $Pd_s2Pd_{sub}Cu_{35}$-II and $Pd_s3Pd_{sub}Cu_{34}$-II, respectively.

For the Cu_{55} and Pd-doped Cu_{55} clusters, Cu_{55} cluster with the icosahedron structure has been experimentally confirmed to be the most stable and high symmetry [54,55]. Cu_{55} cluster has a two-shell centered structure and the shell, the sub-layer and the inner core contain 42, 12 and one Cu atoms, respectively. Obviously, there are two kinds of shell Cu atoms, 6-coordination and 8-coordination. Accordingly, there are two ways to dope the single Pd atom into the outermost layer of Cu_{55}; both are named as Pd_sCu_{54}-I and Pd_sCu_{54}-II corresponding to the coordination numbers of 6 and 8, respectively. Further, for the Pd_sCu_{54}-I, there is only one pattern ($Pd_sPd_{sub}Cu_{53}$-I) with Pd atoms doped into the sub-layer; for the Pd_sCu_{54}-II, one and two sub-layer Cu atoms can be replaced by Pd atoms, both are donated as $Pd_sPd_{sub}Cu_{53}$-II and $Pd_s2Pd_{sub}Cu_{52}$-II, respectively, in which the sub-layer Pd atoms are connected to the individual shell Pd atom.

Cu nano-clusters with much larger size were modeled by a four-layers Cu(111) surface with 3 × 3 supercell because (111) surface is the most stable of close-packed Cu, and all Cu atoms have the coordination number of 9, just like Cu_{147} nano-cluster. Cu(111) surface has been widely used to represent the larger size [32]. In order to simulate the bulk environment of the catalyst under the actual conditions, the bottom two layers of Cu(111) were fixed, the other layers with adsorbed species were relaxed. A 15 Å vacuum was chosen to ensure that the interactions between periodic slabs are negligible. Replacing a surface Cu atom of Cu(111) with a Pd atom can obtain Pd_sCu(111), then, one, two and three Pd atoms are doped into the sub-layer of Pd_sCu(111) to obtain $Pd_sPd_{sub}Cu$(111), $Pd_s2Pd_{sub}Cu$(111) and $Pd_s3Pd_{sub}Cu$(111), respectively.

3. Results and discussion

Firstly, H_2 adsorption and dissociation over the Cu and Pd-doped Cu clusters with different sizes were systematically investigated to explore the relationship of catalytic activity with cluster sizes and Pd ensemble. The adsorption of one H atom on all catalysts is calculated to achieve the most stable adsorption site, as listed in Table S1. The structures of reactants, transition states and products in H_2 dissociation over these catalyst surfaces were presented in Fig. S1. Table 1 lists the distances of H-Pd or H-Cu, the length of H—H bond, the adsorption free energy of H_2, as well as activation barrier and reaction energy for H_2 dissociation on the Cu and Pd-doped Cu clusters.

3.1. H_2 adsorption and dissociation on the pure and Pd-doped Cu_{13} clusters

For the Cu_{13} and Pd-doped Cu_{13} clusters, the preferred adsorption site for H_2 is the top Cu or Pd atoms with a parallel adsorption mode, which have the adsorption free energies of 38.3, 66.0 and 86.5 kJ mol^{-1} over the Cu_{13}, Pd_sCu_{12} and $Pd_sPd_{sub}Cu_{11}$ clusters, respectively; the bond lengths of adsorbed H_2 is obviously increased to 0.815, 0.847 and 0.876 Å compared to 0.748 Å in gaseous H_2, indicating that the H—H bond of H_2 is activated upon its adsorption. Moreover, the activation barriers of H_2 dissociation are 49.0, 41.4 and 23.0 kJ mol^{-1} over the Cu_{13}, Pd_sCu_{12} and $Pd_sPd_{sub}Cu_{11}$, respectively; the reaction energies are −72.9, −63.1 and −48.3 kJ mol^{-1}, respectively.

Table 1
The distances (in Å) of H-Pd or H-Cu, the length of H—H bond, adsorption free energy (G_{ads}/kJ mol^{-1}), activation barrier (ΔG_a/kJ mol^{-1}) and reaction energy (ΔG/kJ mol^{-1}) in the adsorption-dissociation processes of H_2 on different sizes of the Cu and Pd-doped Cu catalysts.

Pd-doped Cu catalysts		$d_{H\text{-}Pd(Cu)}$	$d_{H\text{-}H}$	G_{ads}	ΔG_a	ΔG
Cu_{13}	Cu_{13}	1.702	0.815	38.3	49.0	−72.9
	Pd_sCu_{12}	1.767	0.847	66.0	41.4	−63.1
	$Pd_sPd_{sub}Cu_{11}$	1.733	0.876	86.5	23.0	−48.3
Cu_{38}	Cu_{38}-I	1.860	0.778	26.6	75.3	−38.0
	Pd_sCu_{37}-I	1.826	0.821	50.3	62.9	1.3
	$Pd_sPd_{sub}Cu_{36}$-I	1.799	0.827	51.5	42.3	−4.6
	Cu_{38}-II	1.952	0.777	26.3	70.2	−54.3
	Pd_sCu_{37}-II	1.845	0.821	29.0	31.9	−24.0
	$Pd_sPd_{sub}Cu_{36}$-II	1.819	0.828	33.9	24.3	−28.5
	$Pd_s2Pd_{sub}Cu_{35}$-II	1.810	0.833	35.3	23.8	−19.4
	$Pd_s3Pd_{sub}Cu_{34}$-II	1.802	0.836	37.7	19.8	−15.6
Cu_{55}	Cu_{55}-I	1.855	0.782	23.3	96.4	−21.9
	Pd_sCu_{54}-I	1.862	0.810	38.9	82.3	−42.3
	$Pd_sPd_{sub}Cu_{53}$-I	1.817	0.822	45.9	51.2	−33.6
	Cu_{55}-II	1.873	0.788	18.5	69.6	−16.6
	Pd_sCu_{54}-II	1.821	0.829	39.1	26.7	−23.9
	$Pd_sPd_{sub}Cu_{53}$-II	1.786	0.843	47.6	23.3	−22.0
	$Pd_s2Pd_{sub}Cu_{52}$-II	1.767	0.854	53.2	16.4	−25.2
Cu(111)	Cu(111)	2.789	0.753	20.9	73.9	−25.5
	Pd_sCu(111)	1.832	0.824	22.8	23.1	−30.7
	$Pd_sPd_{sub}Cu$(111)	1.807	0.834	32.4	18.7	−26.7
	$Pd_s2Pd_{sub}Cu$(111)	1.780	0.842	35.2	10.3	−28.9
	$Pd_s3Pd_{sub}Cu$(111)	1.769	0.851	43.2	16.2	−26.9

Fig. 3(a) shows the relationship for the H—H bond length of adsorbed H_2 and the activity of H_2 dissociation as a function of H_2 adsorption free energy over the pure and Pd-doped Cu_{13} cluster, suggesting that with the increasing of doped Pd atom number, the adsorption free energy of H_2 also increases to facilitate H_2 activation, accordingly, the length of H—H bond increases, which decreases the activation barriers of H_2 dissociation.

3.2. H_2 adsorption and dissociation on the pure and Pd-doped Cu_{38} clusters

On the Cu_{38} cluster, H_2 has two types of adsorption sites, one is 6-coordination Cu site (Cu_{38}-I), the other is 9-coordination Cu site (Cu_{38}-II). For the Cu_{38} and Pd-doped Cu_{38} clusters, H_2 also prefers to be adsorbed at the top Cu or Pd sites in a parallel configuration, respectively.

As presented in Fig. 3(c) and (d), with the increasing of doped Pd atoms, the adsorption free energies of H_2 (26.6, 50.3 and 51.5 kJ mol^{-1} on Cu_{38}-I, Pd_sCu_{37}-I, $Pd_sPd_{sub}Cu_{36}$-I, respectively; 26.3, 29.0, 33.9, 35.3 and 37.7 kJ·mol^{-1} on Cu_{38}-II, Pd_sCu_{37}-II, $Pd_sPd_{sub}Cu_{36}$-II, $Pd_s2Pd_{sub}Cu_{35}$-II and $Pd_s3Pd_{sub}Cu_{34}$-II, respectively) and the H—H bond lengths of adsorbed H_2 (0.778, 0.821 and 0.827 Å on Cu_{38}-I, Pd_sCu_{37}-I, $Pd_sPd_{sub}Cu_{36}$-I; 0.777, 0.821, 0.828, 0.833 and 0.836 Å on Cu_{38}-II, Pd_sCu_{37}-II, $Pd_sPd_{sub}Cu_{36}$-II, $Pd_s2Pd_{sub}Cu_{35}$-II and $Pd_s3Pd_{sub}Cu_{34}$-II) increase, namely, the increasing of doped Pd atoms is beneficial for H_2 activation, which decrease its dissociation barriers (75.3, 62.9 and 42.3 kJ mol^{-1} on Cu_{38}-I, Pd_sCu_{37}-I, $Pd_sPd_{sub}Cu_{36}$-I; 70.2, 31.9, 24.3, 23.8 and 19.8 kJ·mol^{-1} on Cu_{38}-II, Pd_sCu_{37}-II, $Pd_sPd_{sub}Cu_{36}$-II, $Pd_s2Pd_{sub}Cu_{35}$-II and $Pd_s3Pd_{sub}Cu_{34}$-II).

On the other hand, H_2 dissociation on the 9-coordination Pd-doped Cu_{38} cluster has lower catalytic activity than that on the 6-coordination Pd-doped Cu_{38} cluster, namely, the shell Cu atom replacement by Pd atom should focus on the 9-coordination Cu, which exhibits higher catalytic activity towards H_2 dissociation.

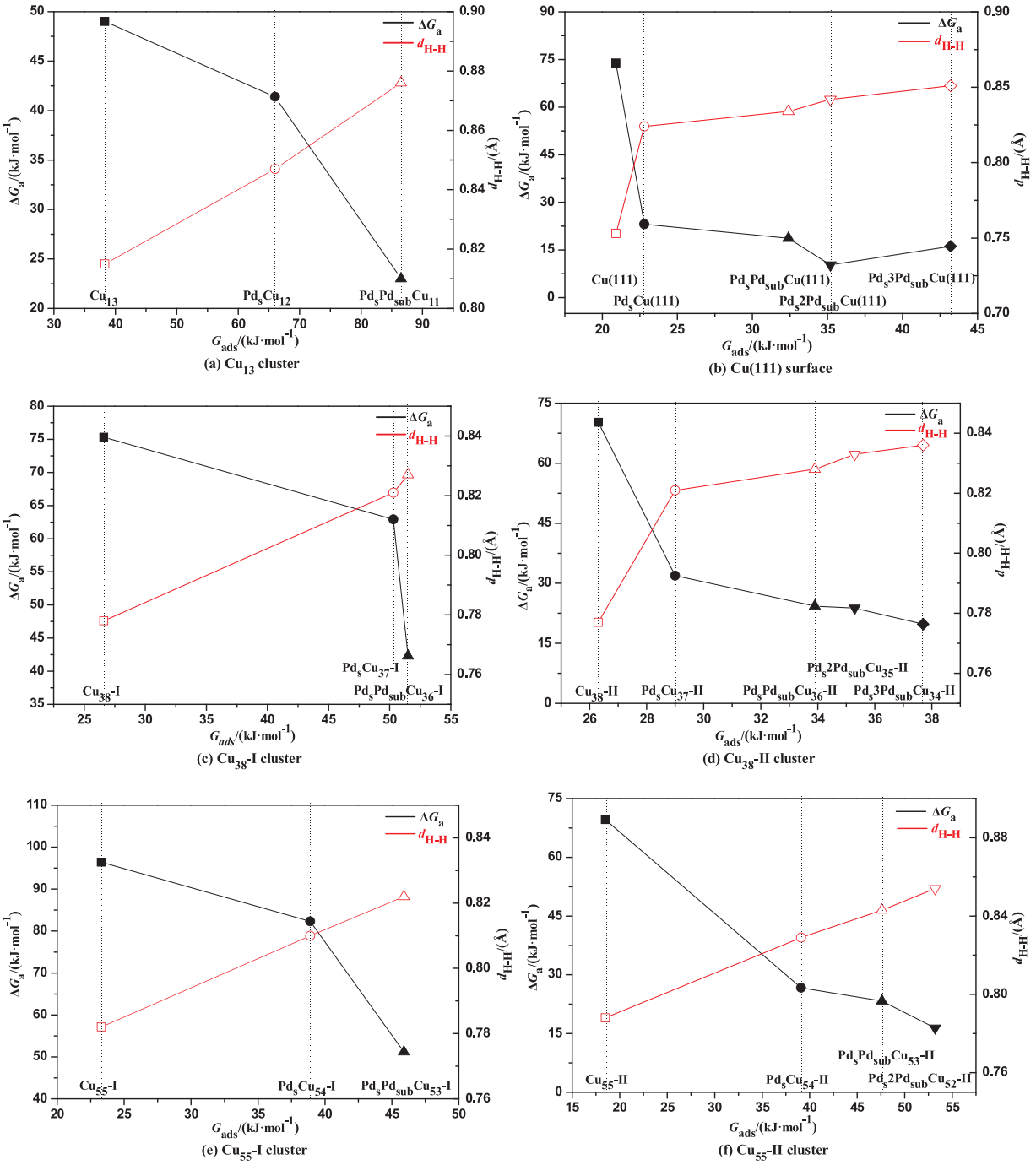

Fig. 3. The relationship for the activation barrier of H_2 dissociation (ΔG_a) and the H—H bond length of adsorbed H_2 ($d_{H\text{-}H}$) as a function of H_2 adsorption free energy (G_{ads}) on different sizes of the Cu and Pd-doped Cu catalysts. (a) Cu_{13} cluster, (b) Cu(111) surface, (c) Cu_{38}-I cluster, (d) Cu_{38}-II cluster, (e) Cu_{55}-I cluster, (f) Cu_{55}-II cluster.

3.3. H_2 adsorption and dissociation on the pure and Pd-doped Cu_{55} clusters

Similarly, on the Cu_{55} and Pd-doped Cu_{55} clusters, H_2 has also two types of adsorption site, one is the Top I with the 6-coordination number, the other is the Top II with the 8-coordination number; at both cases, H_2 is inclined to adsorb at the top Cu or Pd atoms in a parallel configuration. As shown in Fig. 3(e) and (f), with the increasing of doped Pd atoms, the adsorption free energies and the H—H bond lengths of H_2 increase, H_2 activation and dissociation becomes easier. Then, in order to achieve higher activity towards H_2 dissociation, the replacement of shell Cu atom by Pd atom should focus on the 8-coordination Cu instead of the 6-coordination Cu. First-principle work by Cao et al. [56] also confirmed that the Pd atom doped at high-coordination site of Cu_{55} nanoparticle promotes H_2 dissociation remarkably.

3.4. H_2 adsorption and dissociation on the pure and Pd-doped Cu(111) surface

For the Cu(111) periodic surface, the adsorption of H_2 has a weaker interaction (20.9 kJ mol^{-1}) to keep away from Cu(111) surface, which is a typical physisorption. The H—H bond length of 0.753 Å is close to that in gaseous H_2 (0.748 Å). Experimental observations by Tierney et al. [24] also confirmed that the dissociation barrier of H_2 is high on

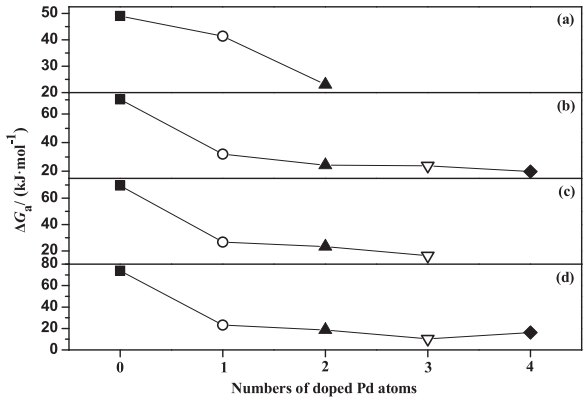

Fig. 4. The change trend for the activation barriers of H_2 dissociation with the number increasing of doped-Pd atoms over different sizes of Cu catalysts. (a) Cu_{13} cluster, (b) Cu_{38} cluster, (c) Cu_{55} cluster, (d) Cu(111) surface.

Cu(111) surface, and its dissociation is not observed.

For the Pd-doped Cu(111), H_2 is more likely to adsorb at the top Pd atom with a parallel mode. See Fig. 3(b), the adsorption free energies of H_2 (22.8, 32.4, 35.2, 43.2 kJ·mol^{-1}) and the H—H bond lengths of adsorbed H_2 (0.824, 0.834, 0.842, 0.851 Å) increase with the increasing of Pd number on $Pd_sCu(111)$, $Pd_sPd_{sub}Cu(111)$, $Pd_s2Pd_{sub}Cu(111)$ and $Pd_s3Pd_{sub}Cu(111)$, accordingly, the activation barriers of H_2 dissociation decrease (23.1, 18.7, 10.3, 16.2 kJ mol^{-1}), this decreasing trend agrees with previous studies [3]; moreover, the Pd-doped Cu(111) surface exhibit stronger catalytic activity towards H_2 dissociation [20,23–25].

3.5. General discussions

3.5.1. The effect of Pd ensemble on the activity

Fig. 4 shows the change trend of H_2 dissociation barrier with the change of Pd number. Compared to Cu catalyst, Pd_s-doped Cu catalyst with one Pd atom at the outermost dramatically reduces H_2 dissociation barrier and increase H_2 dissociation activity. Subsequently, compared to Pd_s-doped Cu catalyst, Pd_snPd_{sub}-doped Cu catalyst with *n*Pd atoms doped into the sub-layer to form Pd ensemble further promote H_2 activation and dissociation. Thus, Pd ensemble as active center formed by the outermost layer and its connected sub-layer Pd atoms exhibits better catalytic activity of H_2 dissociation, which agree with the previous studies [57] that the Pd ensemble formed by surface Pd atom connected with several subsurface Pd atoms of Cu(111) improves the catalytic performance for acetylene hydrogenation to ethylene.

Aiming at further illustrating the microscopic reasons, the *d*-band center for the Cu and Pd-doped Cu catalysts were calculated (Fig. 5). As we all know, upshifting *d*-band center would enhance the ability of adsorbed species with the catalyst [3,56]. As a result, the upshift of *d*-band center towards the Fermi level will enhance the ability H_2 adsorption. On the Cu_{13} cluster (Fig. 5(a)), the adsorption free energy of H_2 is 38.3 kJ·mol^{-1} with the *d*-band center at -2.02 eV. When the Pd atoms are doped into the Cu_{13} cluster, the adsorption free energy of H_2 increases with the upshifting of *d*-band center towards the Fermi level, which favored the activation and dissociation of H_2. For the Cu_{38} and Pd-doped Cu_{38} clusters (Fig. 5(b) and (c)), the *d*-band centers (-2.42, -2.05, -2.03 eV on the Cu_{38}-I, Pd_sCu_{37}-I, $Pd_sPd_{sub}Cu_{36}$-I; -2.62, -2.42, -2.39, -2.37 and -1.54 eV on the Cu_{38}-II, Pd_sCu_{37}-II, $Pd_sPd_{sub}Cu_{36}$-II, $Pd_s2Pd_{sub}Cu_{35}$-II and $Pd_s3Pd_{sub}Cu_{34}$-II) gradually approach the Fermi level with the increasing of doped Pd atoms, the adsorption energies of H_2 increase. Similarly, on the Cu_{55} and Pd-doped Cu_{55} clusters (Fig. 5(d) and (e)), as well as on the periodic Cu(111) and Pd-doped Cu (111) surfaces (Fig. 5(f)), with the increasing of doped Pd atom numbers, the *d*-band center gradually upshifts towards the Fermi level.

As mentioned above, when Pd-doped Cu clusters is at the same size, the increasing of doped Pd atom number makes the *d*-band center of outermost layer Pd atom gradually approach the Fermi level, the adsorption ability of H_2 also increases to facilitate H_2 activation, and H_2 dissociation becomes easier.

Therefore, Pd ensemble consisted of the outermost layer and its connected sub-layer Pd atoms over the Pd-doped Cu catalysts enhance the catalytic activity of H_2 dissociation. It would be highly valuable to synthesize Pd ensemble over the Pd-doped Cu catalysts. Although Pd ensemble is more active, Pd ensemble possibly does not exist due to its higher energy. Interestingly, up to now, for PdCu catalysts, previous experiments [24,25,28] have observed that during the deposition process, a part of Pd atoms goes into the sublayers of Cu(111). Tierney et al. [24,25] found Pd atoms were selectively placed in the surface, subsurface, and bulk of Cu by controlling the temperature. Aaen et al. [28] studied the growth mode of sub-monolayer amounts of Pd on Cu (111) and found an attractive interaction between surface Pd and subsurface Pd. Thus, one to three Pd atoms doped into Cu catalysts are feasible, namely, Pd ensemble can be experimentally realized by a Cu catalyst doped with a very small quantity of Pd into the surface and sublayer to join together thanks to the advances in the process of material synthesis.

3.5.2. The effect of cluster size on the activity

For the Cu_{38} and Cu_{55} clusters, the shell-layer Cu atoms have different coordination numbers to form Pd-doped Cu-I and Pd-doped Cu-II; however, both Cu-II and Pd-doped Cu-II cluster with high coordination number have higher catalytic activity towards H_2 dissociation than Cu-I and Pd-doped Cu-I cluster. Thus, different sizes of Cu_{13}, Cu_{38}-II, Cu_{55}-II, Cu(111), as well as the corresponding Pd-doped Cu were further analyzed to obtain the size effect of nano-cluster on H_2 dissociation.

Fig. 6 reveals the change trend of H_2 dissociation barriers along with the cluster size increasing when the doped Pd atoms have the same number. For the Cu cluster, when the cluster size increases, H_2 dissociation barrier increase generally, thus, the large size Cu cluster is not in favor of H_2 dissociation, whereas the small-sized Cu clusters is more suitable for the dissociation of H_2. Previous theoretical studies by Guvelioglu et al. [58] showed that the small-sized nanoparticles among Cu clusters ($n < 15$) have better catalytic activity for H_2 dissociative chemisorption. However, for the Pd-doped Cu cluster, when the number of doped-Pd atoms is same, overall, H_2 dissociation barrier decrease as the sizes of Cu cluster increase, namely, in the preparation of Pd-doped Cu bimetallic catalysts, the particles size should be kept in a relatively large range, which greatly improves catalytic activity of H_2 dissociation.

Therefore, the size decreasing of Cu clusters and the size increasing of Pd-doped Cu clusters contributes to H_2 dissociation, indicating that the change trend of H_2 dissociation activation barrier is opposite between pure Cu and Pd-doped Cu. To understand the microscopic reasons, we further investigate the geometric and electronic effects of Cu and Pd-doped Cu clusters. The results of Bader charge show that the charge of shell Cu are −0.014, −0.016, −0.018 and −0.017 *e* on the Cu_{13}, Cu_{38}, Cu_{55} and Cu(111), respectively, thus, the charge of shell Cu are essentially the same among the studies clusters, which means that the size effect of pure Cu cluster on H_2 dissociation may be dominantly attributed to the geometric effect. More importantly, in terms of the coordination number of Cu atom, the number of Cu_{13} is 6, while it is 9, 8 and 9 of Cu_{38}-II, Cu_{55}-II and Cu(111), respectively, thus, compared to Cu_{38}-II, Cu_{55}-II cluster and Cu(111) surface, the shell Cu of Cu_{13} cluster has the minimum coordination number with the highest unsaturation leading to the strongest adsorption ability of H_2 and the lowest dissociation barrier of H_2. In addition, experimental and theoretical studies [59,60] have also proved that the size effect of Cu clusters is indeed related to the coordination number of shell Cu atoms and the larger coordination number, the smaller adsorption energy of adsorbed species.

On the other hand, for the Pd-doped Cu catalysts, the charge

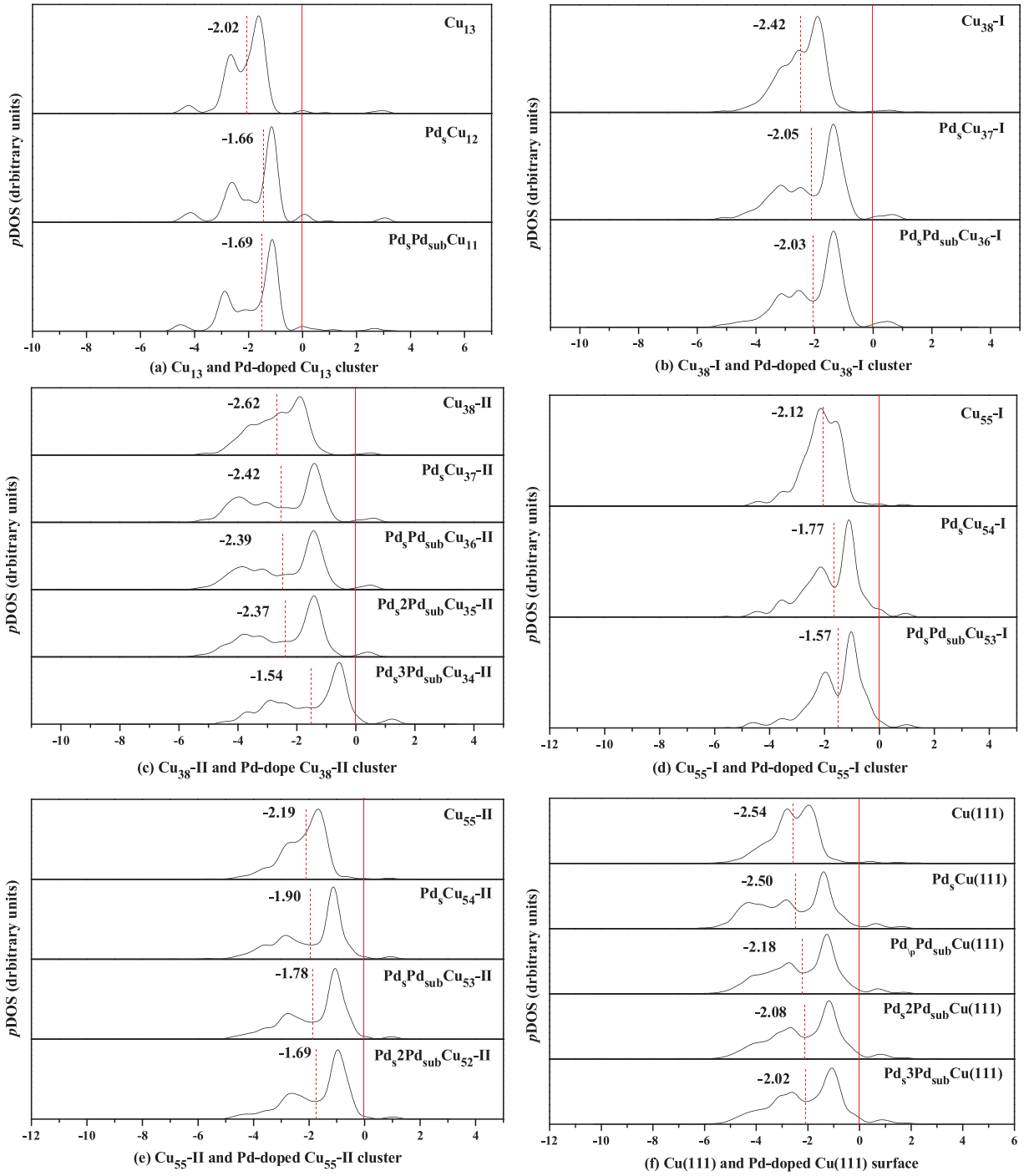

Fig. 5. Projected density of states (*p*DOS) plots of the *d*-orbitals for the pure Cu catalysts and the Pd-doped Cu catalysts. *p*DOS belongs to Cu atoms on the pure Cu catalysts, while that belongs to Pd atoms on the Pd-doped Cu catalysts. (a) Cu_{13} cluster, (b) Cu_{38}-I cluster, (c) Cu_{38}-II cluster, (d) Cu_{55}-I cluster, (e) Cu_{55}-II cluster, (f) Cu(111) surface. The vertical dashed lines represent the location of *d*-band center, and the vertical solid lines indicate Fermi energy level.

transferred from Cu to Pd gradually increases on the Pd_s-doped Cu (-0.184, -0.319, -0.324 and -0.356 *e* on the Pd_sCu_{12}, Pd_sCu_{37}-II, Pd_sCu_{54}-II and $Pd_sCu(111)$, respectively), Pd_sPd_{sub}-doped Cu (-0.444, -0.539, -0.558 and -0.615 *e* on the $Pd_sPd_{sub}Cu_{11}$, $Pd_sPd_{sub}Cu_{36}$-II, $Pd_sPd_{sub}Cu_{53}$-II and $Pd_sPd_{sub}Cu(111)$, respectively), Pd_s2Pd_{sub}-doped Cu (-0.685. -0.735 and -0.843 *e* on the $Pd_s2Pd_{sub}Cu_{35}$-II, $Pd_s2Pd_{sub}Cu_{52}$-II and $Pd_s2Pd_{sub}Cu(111)$, respectively) and Pd_s3Pd_{sub}-doped Cu (-0.819 and -1.043 *e* on the $Pd_s3Pd_{sub}Cu_{34}$-II and $Pd_s3Pd_{sub}Cu(111)$, respectively), respectively. The results of charge transfer indicate that when the number of doped-Pd atoms is same, the amount of charge on Pd ensemble increases with the size increasing of Pd-doped Cu catalysts, which can promote H_2 dissociation easily. Thus, the size effect of Pd-doped Cu cluster on H_2 dissociation is dominantly attributed to the electronic effect.

3.5.3. The analysis of electronic properties

Table 2 lists the Bader charge to further clarify the charge distribution for the Pd-doped Cu catalysts. For the Pd_sCu_{12} cluster, the charge of the shell Pd atom is -0.184 *e*. For the $Pd_sPd_{sub}Cu_{11}$ cluster, the total charge of the shell and inner core Pd atoms are -0.444 *e*. Thus, the doping of Pd atoms causes charge-transfer from Cu to Pd atoms, and the amount of obtained charge is more with the increasing

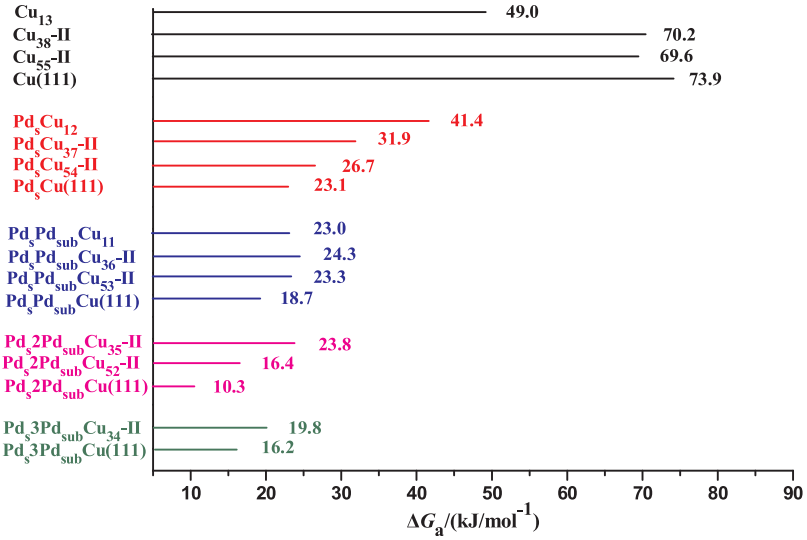

Fig. 6. The change trend of the activation barriers of H_2 dissociation with the increasing of doped Pd atoms when the number of doped Pd atoms is the same. The black, red, blue, pink and green lines correspond to the Cu, Pd_s-doped Cu, Pd_sPd_{sub}-doped Cu, Pd_s2Pd_{sub}-doped Cu and Pd_s3Pd_{sub}-doped Cu catalysts on the different size of the clusters, respectively. (For interpretation of the references to colour in this figure legend, the reader is referred to the web version of this article.)

Table 2
Bader charge (*e*) transferred from Cu atoms to Pd atoms on the different sizes of Pd-doped Cu catalysts.

Pd-doped Cu catalyst	Bader Charge	Pd-doped Cu catalyst	Bader Charge
Pd_sCu_{12}	−0.184	$Pd_sPd_{sub}Cu_{11}$	−0.444
Pd_sCu_{37}-I	−0.268	$Pd_sPd_{sub}Cu_{36}$-I	−0.474
Pd_sCu_{37}-II	−0.319	$Pd_sPd_{sub}Cu_{36}$-II	−0.539
$Pd_s2Pd_{sub}Cu_{35}$-II	−0.685	$Pd_s3Pd_{sub}Cu_{34}$-II	−0.819
Pd_sCu_{54}-I	−0.338	$Pd_sPd_{sub}Cu_{53}$-I	−0.566
Pd_sCu_{54}-II	−0.324	$Pd_sPd_{sub}Cu_{53}$-II	−0.558
$Pd_s2Pd_{sub}Cu_{52}$-II	−0.735	$Pd_sCu(111)$	−0.356
$Pd_sPd_{sub}Cu(111)$	−0.615	$Pd_s2Pd_{sub}Cu(111)$	−0.843
$Pd_s3Pd_{sub}Cu(111)$	−1.043		

of Pd atoms. Similar results are observed on the Pd-doped Cu_{38}-II, Pd-doped Cu_{55}-II and Pd-doped Cu(111), namely, the electron densities of Cu atoms are reduced, whereas Pd atoms form the electron-rich regions, which is beneficial to H_2 activation and the subsequent dissociation. This result is consistent with the order of electronegativity that Pd (2.20) is stronger than that of Cu (1.90) [61]. Plenty of researches have experimentally and theoretically shown that Cu transfer electrons to Pd atoms in PdCu bimetallic catalysts [19,44,62,63]. For example, in the work of Venezia et al. [62], the negative electrons were observed on Pd atoms in pumice-supported Cu-Pd catalysts. Zhang et al. [63] found that surface Pd atoms are the electron aggregation regions, which is the catalytic active center over Pd-Cu alloy catalysts in HCOOH oxidation. Pei et al. [44] demonstrated that charge transfer to Pd from Cu and the electron-rich Pd atoms could enhance ethylene selectivity in the semi-hydrogenation of acetylene. Liu et al. [19] found that the increased electrons of Pd atoms from Cu could promote desorption of ethylene and improve the selectivity in partial hydrogenation of acetylene.

The electron density difference is further examined to illustrate the effect of Pd atoms on the electron distribution of Cu clusters. There are up to three sub-layer Pd atoms are connected with the outmost layer Pd atom on the Pd-doped Cu_{38}-II cluster. Thus, the plot of electron density difference on the Cu_{38}-II and Pd-doped Cu_{38}-II clusters are displayed as an example in Fig. 7, which shows a 2D slice from calculated electron density difference data of catalysts. The electron density difference was calculated with a linear combination of the atomic densities. The value of isosurface was set to be 0.1 electrons /$Å^3$. Compared to the single Cu_{38}-II, the doped Pd atoms into Cu_{38}-II make the charge distribution uneven of Cu_{38} cluster, in which the electron enrichment is near the Pd ensemble. Thus, H_2 molecule is more easily absorbed at the Pd atoms, which can donate electrons to H_2; the Pd ensemble formed by the outermost layer and its connected sub-layer Pd atoms is the actually active center, which presents higher activity for catalyzing H_2 dissociation.

As mentioned above, when Cu cluster is doped by Pd atoms, the charge distribution of Cu cluster becomes uneven because of the charge transfer to Pd from Cu atoms, the doped Pd atoms are negatively charged in the Pd-doped Cu clusters, the more the charge of Pd atoms is, the stronger the catalytic activity of H_2 dissociation is. Thus, although the charge transfer is just the results of doping, it is not directly related to or governs the activation ability; the charge density of doped Pd atoms can be only used to simply reflect the catalytic activity of Pd-doped Cu clusters towards H_2 dissociation.

4. Conclusions

DFT calculations are employed to probe into the effects of cluster size and Pd ensemble as active center on H_2 dissociation over Pd-doped Cu bimetallic cluster, in which H_2 adsorption and dissociation was systematically examined over the Cu and Pd-doped Cu catalysts, including Cu_{13}, Cu_{38}, Cu_{55} cluster and the periodic Cu(111) surface. This study reveals that for the single Cu cluster, the larger the cluster size of the Cu is, the lower the catalytic activity of H_2 dissociation is. However, for the promoter Pd atoms doped into Cu cluster, the larger cluster size has the higher catalytic activity towards H_2 dissociation; namely, when the Pd-doped Cu bimetallic catalysts are prepared, the catalyst particles should be controlled within a relatively large particle size, which significantly improve catalytic activity of H_2 dissociation. On the other hand, the promoter Pd ensemble formed by the outermost layer and its connected sub-layer as active center promote the adsorption, activation and dissociation of H_2, which is attributed to that the *d*-band centers gradually approach the Fermi level and the doped Pd atoms make the charge distribution uneven of Cu cluster due to the charge transfer from Cu to Pd. The more the charge of Pd atoms is, the stronger the activity of H_2 dissociation is. Thus, controlling the catalyst particle size and the promoter Pd ensemble in heterogeneous hydrogenation are useful ways to enhance the catalytic activity of H_2 dissociation over the Pd-doped Cu catalysts.

Acknowledgments

This work is financially supported by the Key Project of National Natural Science Foundation of China (No. 21736007), National Natural Science Foundation of China (No. 21776193, 21476155), the Program for the Top Young Academic Leaders of Higher Learning Institutions of Shanxi, and the Top Young Innovative Talents of Shanxi.

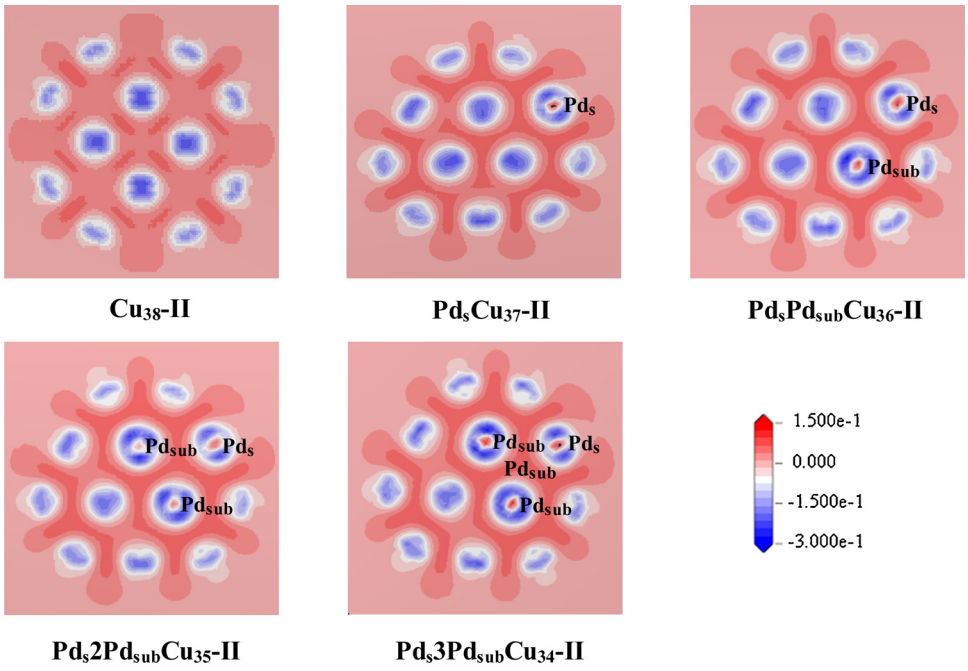

Fig. 7. The plot of electron density difference for the Cu_{38}-II and Pd-doped Cu_{38}-II clusters calculated with a linear combination of the atomic densities, the value of isosurface was set to be 0.1 electrons /Å^3. The loss of electrons and the electron enrichment are indicated in the blue and red color, respectively. (For interpretation of the references to colour in this figure legend, the reader is referred to the web version of this article.)

Appendix A. Supplementary data

Supplementary material related to this article can be found, in the online version, at doi:https://doi.org/10.1016/j.mcat.2019.110457.

References

[1] A.J. Mccue, A.M. Shepherd, J.A. Anderson, Optimisation of preparation method for Pd doped Cu/Al_2O_3 catalysts for selective acetylene hydrogenation, Catal. Sci. Technol. 5 (2015) 2880–2890.

[2] J.W.A. Sachtler, G.A. Somorjai, Influence of ensemble size on CO chemisorption and catalytic n-hexane conversion by Au-Pt(111) bimetallic single-crystal surfaces, J. Catal. 81 (1983) 77–94.

[3] Q. Fu, Y. Luo, Active Sites of Pd-doped flat and stepped Cu(111) surfaces for H_2 dissociation in heterogeneous catalytic hydrogenation, ACS Catal. 3 (2013) 1245–1252.

[4] U. Schneider, H. Busse, R. Linke, G.R. Castro, K. Wandelt, Interaction properties of molecules with binary alloy surfaces, J. Vac. Sci. Technol. A 12 (1994) 2069–2073.

[5] N. Kristian, Y. Yan, X. Wang, Highly efficient submonolayer Pt-decorated Au nanocatalysts for formic acid oxidation, Chem. Commun. 3 (2008) 353–355.

[6] M. Neurock, M. Janik, A. Wieckowski, A first principles comparison of the mechanism and site requirements for the electrocatalytic oxidation of methanol and formic acid over Pt, Faraday Discuss. 140 (2008) 363–378.

[7] D.W. Yuan, X.G. Gong, R.Q. Wu, Decomposition pathways of methanol on the PtAu (111) bimetallic surface: a first-principles study, J. Chem. Phys. 128 (2008) 064706-1 – 5.

[8] T. Duan, R.G. Zhang, L.X. Ling, B.J. Wang, Insights into the effect of Pt atomic ensemble on HCOOH oxidation over Pt-decorated Au bimetallic catalyst to maximize Pt utilization, J. Phys. Chem. C 120 (2016) 2234–2246.

[9] D.W. Yuan, Z.R. Liu, Atomic ensemble effects on formic acid oxidation on PdAu electrode studied by first-principles calculations, J. Power Sources 224 (2013) 241–249.

[10] J.W. Hong, D. Kim, Y.W. Lee, M. Kim, S.W. Kang, S.W. Han, Atomic-distribution-dependent electrocatalytic activity of Au-Pd bimetallic nanocrystals, Angew. Chem. Int. Ed. 50 (2011) 8876–8880.

[11] X. Jiang, N. Koizumi, X.W. Guo, C.S. Song, Bimetallic Pd–Cu catalysts for selective CO_2 hydrogenation to methanol, Appl. Catal. B: Environ. 170 – 171 (2015) 173–185.

[12] S.X. Bai, Q. Shao, P.T. Wang, Q.G. Dai, X.Y. Wang, X.Q. Huang, Highly active and selective hydrogenation of CO_2 to ethanol by ordered Pd-Cu nanoparticles, J. Am. Chem. Soc. 139 (2017) 6827–6830.

[13] X.W. Nie, X. Jiang, H.Z. Wang, W.J. Luo, M.J. Janik, Y.G. Chen, X.W. Guo, C.S. Song, Mechanistic understanding of alloy effect and water promotion for Pd-Cu bimetallic catalysts in CO_2 hydrogenation to methanol, ACS Catal. 8 (2018) 4873–4892.

[14] M. Gupta, M.L. Smith, J.J. Spivey, Heterogeneous catalytic conversion of dry syngas to ethanol and higher alcohols on Cu-based catalysts, ACS Catal. 1 (2011) 641–656.

[15] Z.J. Zuo, F. Peng, W. Huang, Efficient synthesis of ethanol from CH_4 and syngas on a Cu-Co/TiO_2 catalyst using a stepwise reactor, Sci. Rep. 6 (2016) 34670.

[16] J.H. Lee, K.H. Reddy, J.S. Jung, E.H. Yang, D.J. Moon, Role of support on higher alcohol synthesis from syngas, Appl. Catal. A Gen. 480 (2014) 128–133.

[17] A.J. Mccue, C.J. Mcritchie, A.M. Shepherd, J.A. Anderson, Cu/Al_2O_3 catalysts modified with Pd for selective acetylene hydrogenation, J. Catal. 319 (2014) 127–135.

[18] C.M. Kruppe, J.D. Krooswyk, M. Trenary, Selective hydrogenation of acetylene to ethylene in the presence of a carbonaceous surface layer on a Pd/Cu(111) single-atom alloy, ACS Catal. 7 (2017) 8042–8049.

[19] Y.N. Liu, Y.F. He, D.R. Zhou, J.T. Feng, D.Q. Li, Catalytic performance of Pd-promoted Cu hydrotalcite-derived catalysts in partial hydrogenation of acetylene: effect of Pd-Cu alloy formation, Catal. Sci. Technol. 6 (2016) 3027–3037.

[20] M. Ramos, A.E. Martínez, H.F. Busnengo, H_2 dissociation on individual Pd atoms deposited on Cu(111), Phys. Chem. Chem. Phys. 14 (2012) 303–310.

[21] G. Kyriakou, E.R.M. Davidson, G.W. Peng, L.T. Roling, S. Singh, M.B. Boucher, M.D. Marcinkowski, M. Mavrikakis, A. Michaelides, E.C.H. Sykes, Significant quantum effects in hydrogen activation, ACS Nano 8 (2014) 4827–4835.

[22] J.A. Santana, N. Rösch, Hydrogen adsorption on and spillover from Au- and Cu-supported Pt_3 and Pd_3 clusters: a density functional study, Phys. Chem. Chem. Phys. 14 (2012) 16062–16069.

[23] G. Kyriakou, M.B. Boucher, A.D. Jewell, E.A. Lewis, T.J. Lawton, A.E. Baber, H.L. Tierney, M. Flytzani-Stephanopoulos, E.C. Sykes, Isolated metal atom geometries as a strategy for selective heterogeneous hydrogenations, Science 335 (2012) 1209–1212.

[24] H.L. Tierney, A.E. Baber, E.C.H. Sykes, Atomic-scale imaging and electronic structure determination of catalytic sites on Pd/Cu near surface alloys, J. Phys. Chem. C 113 (2009) 7246–7250.

[25] H.L. Tierney, A.E. Baber, J.R. Kitchin, E.C.H. Sykes, Hydrogen dissociation and spillover on individual isolated palladium atoms, Phys. Rev. Lett. 103 (2009) 246102-1 – 4.

[26] R.J. Liu, P.A. Crozier, C.M. Smith, D.A. Hucul, J. Blackson, G. Salaita, Metal sintering mechanisms and regeneration of palladium/alumina hydrogenation catalysts, Appl. Catal. A Gen. 282 (2005) 111–121.

[27] B. Yang, R. Burch, C. Hardacre, G. Headdock, P. Hu, Origin of the increase of activity and selectivity of nickel doped by Au, Ag, and Cu for acetylene hydrogenation, ACS Catal. 2 (2012) 1027–1032.

[28] A.B. Aaen, E. Laegsgaard, A.V. Ruban, I. Stensgaard, Submonolayer growth of Pd on Cu(111) studied by scanning tunneling microscopy, Surf. Sci. 408 (1998) 43–56.

[29] J.N. Li, M. Pu, C.C. Ma, Y. Tian, J. He, D.G. Evans, The effect of palladium clusters (Pd_n, n = 2-8) on mechanisms of acetylene hydrogenation: a DFT study, J. Mol. Catal. A Chem. 359 (2012) 14–20.

[30] J. Jia, K. Haraki, J.N. Kondo, A.K. Domen, K. Tamaru, Selective hydrogenation of acetylene over Au/Al_2O_3 catalyst, J. Phys. Chem. B 104 (2000) 11153–11156.

[31] Z.J. Zuo, L. Wang, P.D. Han, W. Huang, Insight into the size effect on methanol decomposition over Cu-based catalysts based on density functional theory, Comput. Theor. Chem. 1033 (2014) 14–22.

[32] B. Zhao, R.G. Zhang, Z.X. Huang, B.J. Wang, Effect of the size of Cu clusters on selectivity and activity of acetylene selective hydrogenation, Appl. Catal. A Gen. 546 (2017) 111–121.

[33] R.G. Zhang, M. Peng, T. Duan, B.J. Wang, Insight into size dependence of C_2 oxygenate synthesis from syngas on Cu cluster: the effect of cluster size on the selectivity, Appl. Surf. Sci. 407 (2017) 282–296.

[34] A.S. Wörz, K. Judai, S. Abbet, U. Heiz, Cluster size-dependent mechanisms of the CO + NO reaction on small Pd_n($n \leq 30$) clusters on oxide surfaces, J. Am. Chem. Soc.

125 (2003) 7964–7970.
[35] S. Kunz, F.F. Schweinberger, V. Habibpour, M. Röttgen, C. Harding, M. Arenz, U. Heiz, Temperature dependent CO oxidation mechanisms on size-selected clusters, J. Phys. Chem. C 114 (2010) 1651–1654.
[36] X.J. Liu, D.X. Tian, C.G. Meng, DFT study on the adsorption and dissociation of H_2 on Pd_n(n = 4, 6, 13, 19, 55) clusters, J. Mol. Struct. 1080 (2015) 105–110.
[37] B. Delley, An all-electron numerical method for solving the local density functional for polyatomic molecules, J. Chem. Phys. 92 (1990) 508–517.
[38] B. Delley, From molecules to solids with the $Dmol^3$ approach, J. Chem. Phys. 113 (2000) 7756–7764.
[39] D.X. Tian, H.L. Zhang, J.J. Zhao, Structure and structural evolution of Ag_n (n = 3-22) clusters using a genetic algorithm and density functional theory method, Solid State Commun. 144 (2007) 174–179.
[40] B. Hammer, L.B. Hansen, J.K. Nørskov, Improved adsorption energetics within density-functional theory using revised Perdew-Burke-Ernzerhof functionals, Phys. Rev. B 59 (1999) 7413–7421.
[41] J.F. Paul, P. Sautet, Influence of the surface atom metallic coordination in the adsorption of ethylene on a platinum surface: a theoretical study, J. Phys. Chem. 98 (1994) 10906–10912.
[42] L. Zhang, W. Li, Molecular dynamics investigation to indicate facet effects on coalescence processes of two copper clusters with different structures, Comput. Mat. Sci. 51 (2012) 91–95.
[43] G.X. Pei, X.Y. Liu, M.Q. Chai, A.Q. Wang, T. Zhang, Isolation of Pd atoms by Cu for semi-hydrogenation of acetylene: effects of Cu loading, Chin. J. Catal. 38 (2017) 1540–1548.
[44] G.X. Pei, X.Y. Liu, X.F. Yang, L.L. Zhang, A.Q. Wang, L. Li, H. Wang, X.D. Wang, T. Zhang, Performance of Cu-alloyed Pd single-atom catalyst for semihydrogenation of acetylene under simulated Front-End Conditions, ACS Catal. 7 (2017) 1491–1500.
[45] A. Canzian, H.O. Mosca, G. Bozzolo, Surface alloying of Pd on Cu(111), Surf. Sci. 551 (2004) 9–22.
[46] A. Roudgar, A. Groß, Hydrogen adsorption energies on bimetallic overlayer systems at the solid–vacuum and the solid–liquid interface, Surf. Sci. 597 (2005) 42–50.
[47] E. Fernández, M. Boronat, A. Corma, Trends in the reactivity of molecular O_2 with copper clusters: influence of size and shape, J. Phys. Chem. C 119 (2015) 19832–19846.
[48] W.Y. Li, F.Y. Chen, A density functional theory study of structural, electronic, optical and magnetic properties of small Ag–Cu nanoalloys, J. Nanopart. Res. 15 (2013) 1809-1 – 14.
[49] K. Shin, D.H. Kim, S.C. Yeo, H.M. Lee, Structural stability of AgCu bimetallic nanoparticles and their application as a catalyst: a DFT study, Catal. Today 185 (2012) 94–98.
[50] M. Kabir, A. Mookerjee, A.K. Bhattacharya, Structure and stability of copper clusters: a tight-binding molecular dynamics study, Phys. Rev. A 69 (2004) 043203.
[51] J.A. Rodriguez, P. Liu, X. Wang, W. Wen, J. Hanson, J. Hrbek, M. Pérez, J. Evans, Water-gas shift activity of Cu surfaces and Cu nanoparticles supported on metal oxides, Catal. Today 143 (2009) 45–50.
[52] Y. Yang, J. Evans, J.A. Rodriguez, M.G. White, P. Liu, Fundamental studies of methanol synthesis from CO_2 hydrogenation on Cu(111), Cu clusters, and Cu/ZnO (000), Phys. Chem. Chem. Phys. 12 (2010) 9909–9917.
[53] S. Núñez, R.L. Johnston, Structures and chemical ordering of small Cu – Ag clusters, J. Phys. Chem. C 114 (2010) 13255–13266.
[54] H. HäKkinen, M. Moseler, O. Kostko, N. Morgner, M.A. Hoffmann, B.V. Issendorff, Symmetry and electronic structure of noble-metal nanoparticles and the role of relativity, Phys. Rev. Lett. 93 (2004) 093401-1 – 4.
[55] T. Rapps, R. Ahlrichs, E. Waldt, M.M. Kappes, D. Schooss, On the structures of 55-atom transition-metal clusters and their relationship to the crystalline bulk, Angew. Chem. Int. Ed. 52 (2013) 6102–6105.
[56] X.R. Cao, Q. Fu, Y. Luo, Catalytic activity of Pd-doped Cu nanoparticles for hydrogenation as a single-atom-alloy catalyst, Phys. Chem. Chem. Phys. 16 (2014) 8367–8375.
[57] R.G. Zhang, B. Zhao, L.X. Ling, A.J. Wang, C.K. Russell, B.J. Wang, M.F. Fan, Cost-effective palladium-doped Cu bimetallic materials to tune selectivity and activity by using doped atom ensembles as active sites for efficient removal of acetylene from ethylene, ChemCatChem 10 (2018) 2424–2432.
[58] G.H. Guvelioglu, P.P. Ma, X.Y. He, First principles studies on the growth of small Cu clusters and the dissociative chemisorption of H_2, Phys. Rev. B 73 (2006) 155436-1–10.
[59] Y.F. Bu, M. Zhao, G.X. Zhang, X.G. Zhang, W. Gao, Q. Jiang, Electro-reduction of CO_2 on Cu clusters: the effects of size, symmetry, and temperature, ChemElectroChem. 6 (2019) 1831–1837.
[60] R. Reske, H. Mistry, F. Behafarid, B.R. Cuenya, P. Strasser, Particle size effects in the catalytic electroreduction of CO_2 on Cu nanoparticles, J. Am. Chem. Soc. 136 (2014) 6978–6986.
[61] R.E. Dickerson, H.B. Gray, G.P. Haight, Chemical Principles, 3rd edition, Benjamin/Cummings Publishing, 1979.
[62] A.M. Venezia, L.F. Liotta, G. Deganello, Z. Schay, L. Guczi, Characterization of pumice-supported Ag-Pd and Cu-Pd bimetallic catalysts by X-Ray photoelectron spectroscopy and X-Ray diffraction, J. Catal. 182 (1999) 449–455.
[63] R.G. Zhang, M. Yang, M. Peng, L.X. Ling, B.J. Wang, Understanding the role of Pd: Cu ratio, surface and electronic structures in Pd-Cu alloy material applied in direct formic acid fuel cells, Appl. Surf. Sci. 465 (2019) 730–739.